

Buckling analysis of structures under combined loading with acceleration forces

Wenjing Wang^{1a} and Randy Gu^{*2}

¹*School of Mechanical, Electric and Control Engineering, Beijing Jiaotong University, Beijing, 10004, China*

²*Department of Mechanical Engineering, Oakland University, Rochester, Michigan 48309, USA*

(Received July 28, 2013, Revised October 23, 2014, Accepted October 27, 2014)

Abstract. The structures of concern in this study are subject to two types of forces: dead loads from the acceleration imposed on the structures as well as the installed operation machines and the additional adjustable forces. We wish to determine the critical values of the adjustable forces when buckling of the structures occurs. The mathematical statement of such a problem gives rise to a constrained eigenvalue problem (CEVP) in which the dominant eigenvalue is subject to an equality constraint. A numerical algorithm for solving the CEVP is proposed in which an iterative method is employed to identify an interval embracing the target eigenvalue. The algorithm is applied to four engineering application examples finding the critical loads of a fixed-free beam subject to its own body force, two plane structures and one wide-flange beam using shell elements when acceleration force is present. The accuracy is demonstrated using the first example whose classical solution exists. The significance of the equality constraint in the EVP is shown by comparing the solutions without the constraint on the eigenvalue. Effectiveness and accuracy of the numerical algorithm are presented.

Keywords: buckling; equality constraint; eigenvalue; acceleration; dead loads; participation factor; finite element; stability

1. Introduction

Buckling has been one of the main concerns in structure design against catastrophic failure for a long time. Naturally the topic has attracted a large group of researchers and engineers in the past rendering a rich source of articles in the area. A few textbooks in theoretical settings as well as numerical practices have been published and used in academia, such as Chajes (1974), Timoshenko and Gere (2009), Bathe (1996), Cook *et al.* (2007), which provide a good source of references in the related fields. Further, the numerical procedures of finding the buckling loads have been implemented in a few commercial codes for engineering practices, for example, ANSYS (ANSYS Inc. 2012), ADINA (ADINA R & D Inc. 2012), MARC (MSC Software 2013), and ABAQUS (Simulia 2011). The study regarding the buckling of the elastic object subject to gravity as well as other applied loads has received much less attention. Roberts and Azizian

*Corresponding author, Professor, E-mail: gu@oakland.edu

^aAssociate Professor, E-mail: wjwang@bjtu.edu.cn

(1984), Roberts and Burt (1985) investigate the lateral buckling of an elastic I-beam subject to uniformly distributed load using energy method. Influence of such parameters as sectional warping rigidity, location of applied load with respect to the shear center is thoroughly studied. Dougherty (1990, 1991) considers the lateral buckling of an elastic beam subject to uniformly distributed load as well as a central point load and end moments. In the studies, gravity load of the beam is modeled as a uniformly distributed load applied on the top surface of the beam. A numerical approach is employed to solve for the critical load for the beam.

The loads applied on the beam in the studies by Kerstens (2005), Cheng *et al.* (2005) appear to be proportional in that the point force and the uniformly distributed load, for example, vary at the same rate, if necessary. In the current study, gravitational load and other applied forces are non-proportional. Thus the buckling problem under the influence of gravity is formulated as a constrained eigenvalue problem. Kerstens (2005) provides a review of methods employed in solving constrained eigenvalue problems. Cheng *et al.* (2005) present a classic study of the buckling of a thin circular plate. In the study, Ritz method is employed to solve the first buckling load of the circular plate with boundary fixed. The only load considered is the in-plane gravity. Kumar and Healey (2010) present a study of stability of elastic rods. The generalized eigenvalue problem consists of a set of constraint equations imposed on the nodal displacements of the model. There is no constraint on the eigenvalue itself. Efficient numerical methods are presented to solve the first few lowest natural eigenvalues. Zhou (1995) examines an algorithm for the design optimization of structure systems subject to both displacement as well as eigenvalue (natural frequency) constraints. An iterative algorithm based on Rayleigh Quotient approximation is shown to be efficient in solving the dual constraint eigenvalue problems.

More recently, Wang *et al.* (2007) investigate the buckling of multi-walled carbon nanotube structure subject to a combined loading of torsion and axial loading. It is found in their study that the buckling mode is different from those under axial compressive force only. Yanagisawa *et al.* (2008) present experimental as well as analytical results of the vibration of a fixed-hinged beam under a compressive axial force and a periodic lateral acceleration. Numerical methods are employed to solve the nonlinear differential equations for chaotic response of the beam yielding results close to the experimental observations. The chaos is believed to be closely related to the buckling load of the beam under an axial compressive load. In the experimental study by Yamada *et al.* (2013) to gain insight of the post buckling of rectangular hollow section (RHS) columns, tests of the columns subject to constant axial force and cyclic bi-directional horizontal loading in analogy to a seismic excitation are conducted. Experimental results are compared with those obtained analytically. Hernandez-Urrea *et al.* (2014) present a parametric stability study of a cantilever structure with multiple masses attached at the ends and axially loaded. It is pointed out from their findings that the attached lumped masses play an important role on the structure stability. The work dealt by Carrera *et al.* (2011) shows the finite element formulations of the vibration and buckling of plates subject to combined in-plane axial and shearing loading. Good accuracy of numerical results comparing with classical solution for thin plates is reported. On the biomimetic front, Cui and Shen (2011) model the plant stems as a stiffened multi-walled cylindrical shell. The model is then subject to various combined loadings including wind pressure, axial compression and bending moment. To determine the buckling load, a commercial FE software package is employed. They conclude that wind pressure has a more profound effect on the buckling of the plant stems subject to bending than axial compression. Silvestre *et al.* (2012) recently propose a multilevel approach to evaluate the buckling of carbon nanotubes embedded in composites. For the buckling analysis they employ the semi-analytical finite strip method. In the

aforementioned studies multiple loads are applied and increased proportionally until buckling occurs.

In this paper, the problem to be tackled is formulated in mathematical form in Section 2. The deviation of the current problem from the others is disclosed. It is shown that addressing the current problem using the usual treatment would lead to significant errors. Section 3 presents a simple algorithm for solving the problem efficiently. The proposed algorithm is tested using four numerical examples in Section 4. It is seen from the examples that the proposed algorithm has achieved excellent accuracy.

2. Mathematical statement of the current problem

Conventionally the buckling load of a structure can be determined by solving the following eigenvalue problem.

$$[\mathbf{K} + \lambda \mathbf{K}_f] \mathbf{U} = \mathbf{0}. \quad (1)$$

where \mathbf{K} is the usual stiffness matrix of the structure, λ the eigenvalue or load factor (LF), \mathbf{U} the nodal displacement vector, and \mathbf{K}_f the stiffness matrix of the same structure due to stress stiffening from an externally applied force f set at an arbitrary reference magnitude. The stress stiffening matrix is given as follows.

$$\mathbf{K}_f = \int \mathbf{G}^T \mathbf{S} \mathbf{G} dV \quad (2)$$

where \mathbf{G} and \mathbf{S} are, respectively, modified strain-displacement and stress matrices (Bathe 1996, Cook *et al.* 2007). Note that in case of line elements, the stress matrix contains only a component $\mathbf{S} = [\sigma_x]$ where σ_x is the axial stress in the elements. Thus, Eq. (2) becomes

$$\mathbf{K}_f = \int \mathbf{G}^T \sigma_x \mathbf{G} dV \quad (3)$$

Likewise, the higher-order Green-strain-displacement matrix for line elements is given as below.

$$\mathbf{G} = \frac{d}{dx} \mathbf{N} \quad (4)$$

where the shape function matrix \mathbf{N} contains the usual linear and cubic Hermitian interpolation functions for bar and beam elements, respectively (Cook *et al.* 2007).

It is understood that for a non-trivial solution to exist, the determinant of the multiplier matrix in Eq. (1) must be zero.

$$\|[\mathbf{K} + \lambda \mathbf{K}_f]\| = \mathbf{0}. \quad (5)$$

Once the eigenvalues are found, the critical buckling load f_c of the structure is given as follows.

$$f_c = \lambda_1 f \quad (6)$$

where λ_1 is the lowest eigenvalue known as critical load factor.

As depicted in Fig. 1, a deformable object is loaded with a reference force f while being subject to a given acceleration motion a_0 . As a result, there are two stress stiffening matrices due to the applied load and the acceleration force, \mathbf{K}_f and \mathbf{K}_{a_0} , respectively. It is our goal to determine the

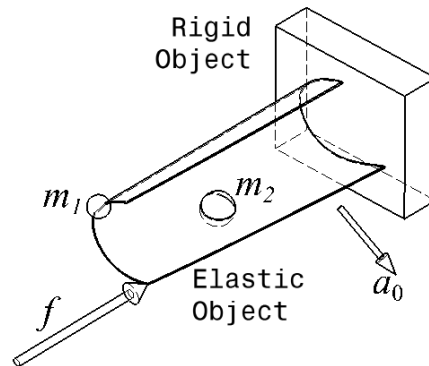


Fig. 1 Schematic of the present problem involving a flexible structure subject to both external force f and acceleration a

buckling load of the structure while it is under the given acceleration. Thus for the current problem an eigenvalue system to be solved may be given below.

$$[\mathbf{K} + \lambda(\mathbf{K}_f + \mathbf{K}_{a0})]\mathbf{U} = \mathbf{0} \quad (7)$$

After the eigenvalue problem is solved, the critical buckling load of the structure can be determined using Eq. (6). Meanwhile, there would be a “critical acceleration” which in combination with the critical load would put the structure in an unstable state. The acceleration under the critical condition a_c is determined via the following relation.

$$a_c = \lambda_1 a_0. \quad (8)$$

Unless $\lambda_1=1$, we have $a_c \neq a_0$. Clearly, the above methodology does not provide the correct solution to the problem. To resolve the issue, it is suggested by ANSYS (ANSYS Inc. 2012) that the problem, Eq. (7), be solved by using the actual acceleration a_0 and iterating the magnitude of f until the load factor is equal to 1, or, $\lambda_1=1$.

Consequently a proper method is required to solve the eigenvalue problem so that the acceleration remains at the fixed value a_0 when buckling occurs. Consider the following constrained eigenvalue problem (CEVP).

$$[\mathbf{K} + \lambda(\mathbf{K}_f + \alpha\mathbf{K}_a)]\mathbf{U} = \mathbf{0} \quad (9)$$

subject to

$$\alpha\lambda_1 = a_0 \quad (10)$$

where \mathbf{K} , \mathbf{K}_f are the same matrices as before, \mathbf{K}_a the stress stiffening matrix using a reference acceleration a , and α an *unknown* participation factor. Of concern is the buckling load f_c of the structure while the acceleration remains at a_0 . Since a is a reference number, we may choose $a=1$ for convenience.

Note that other constrained eigenvalue problem exists in the form given below (Kerstens 2005, Kumar and Healey 2010).

$$\begin{bmatrix} \mathbf{A} & \mathbf{B}^T \\ \mathbf{B} & \mathbf{0} \end{bmatrix} \begin{Bmatrix} \mathbf{U} \\ \mathbf{V} \end{Bmatrix} = \lambda \begin{bmatrix} \mathbf{C} & \mathbf{0} \\ \mathbf{0} & \mathbf{0} \end{bmatrix} \begin{Bmatrix} \mathbf{U} \\ \mathbf{V} \end{Bmatrix}. \quad (11)$$

Or

$$\mathbf{A}\mathbf{U} + \mathbf{B}^T\mathbf{V} = \lambda\mathbf{C}\mathbf{U} \tag{12}$$

subject to

$$\mathbf{B}\mathbf{U} = 0. \tag{13}$$

The above problem sees its applications in determination of the vibration modes of a structure when there are a few equality constraints imposed on the eigenvectors so some nodal displacements in the model are deformed in a specific way. As opposed to this type of problem, the constraint is on the eigenvalue for the current CEVP.

3. Numerical algorithm

For a given structure, the total stiffness matrix \mathbf{K} can be readily formed first. The stress stiffening matrix \mathbf{K}_f can be obtained by using the stress stemming from an arbitrarily chosen reference force f corresponding to the applied load which remains the same throughout the following numerical scheme. To obtain the stress stiffening matrix \mathbf{K}_a due to acceleration, we may choose $a=1$ for convenience. In the following numerical scheme, a series of values for the participation factor α_i is used in solving the following eigenvalue problem.

$$[\mathbf{K} + \lambda(\mathbf{K}_f + \alpha_i\mathbf{K}_a)]\mathbf{U} = \mathbf{0} \tag{14}$$

Therefore, a series of acceleration a_i is obtained via the following relation.

$$\alpha_i\lambda_1 = a_i \tag{15}$$

In the scheme seen in Fig. 2, the eigenproblem is solved until the target value a_0 falls within the interval: $a_i \leq a_0 \leq a_{i+1}$.

Let us introduce a natural coordinate ξ , $-1 \leq \xi \leq +1$. From the following linear interpolation, we can determine the natural coordinate ξ corresponding to the target value a_0 .

$$a_0 = \frac{1}{2}(1 - \xi)a_i + \frac{1}{2}(1 + \xi)a_{i+1}. \tag{16}$$

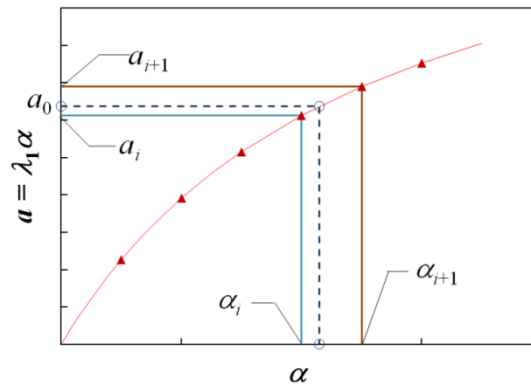


Fig. 2 The trapping scheme for finding unknown α

```

Select values for parameters  $f$ ,  $\alpha_0$ ,  $\Delta\alpha$ 
Guess a starting value for  $\alpha$ .
Form matrices  $\mathbf{K}$ ,  $\mathbf{K}_f$ ,  $\mathbf{K}_a$ 
LOOP STARTS
Set  $\alpha_1=\alpha$ ,  $\alpha_2=\alpha$ ,  $\Lambda_1=\Lambda_2=0$  and
FOUND = FALSE
Solve eigenvalue problem, Eq. (14)
If not FOUND
     $\alpha_1=\alpha_2$ ,  $\Lambda_1=\Lambda_2$ ,  $\Lambda_2=\lambda_1$ 
    If  $\alpha\lambda_1 > a_0$ 
        If  $\Lambda_1=0$ 
             $\alpha = \alpha/2$ ,  $\Delta\alpha = \Delta\alpha/2$ 
        Else
             $\alpha_2=\alpha$ ,  $\Lambda_2=\lambda_1$ 
            Find  $\xi$  using Eq. (17)
            Find  $\alpha$  using Eq. (18)
            FOUND = TRUE
        End If
    Else
         $\alpha = \alpha + \alpha/2$ ,  $\alpha_2 = \alpha$ 
    End If
Else (FOUND critical  $\alpha$ )
    Calculate buckling force  $f_c = \lambda_1 f$ 
    STOP
End If
LOOP ENDS

```

Fig. 3 Pseudo code for the proposed numerical algorithm

Or

$$\xi = (2a_0 - a_i - a_{i+1})/(-a_i + a_{i+1}). \quad (17)$$

Upon substituting this natural coordinate into the following interpolation equation, the unknown participation factor can be determined.

$$\alpha = \frac{1}{2}(1 - \xi)\alpha_i + \frac{1}{2}(1 + \xi)\alpha_{i+1}. \quad (18)$$

It is worth mentioning that linear interpolation is used in the above calculation with a proper selection of the increment used in α_i . The result obtained certainly can be improved if quadratic interpolation is used.

The eigenproblem Eq. (9) is solved one more time using the participation factor found from Eq. (18). The eigenvalue found together with the participation factor in Eq. (18) constitute the solution to the constrained eigenvalue problem. The algorithm of this numerical scheme is given in pseudo code in Fig. 3. The proposed algorithm can be easily implemented in ANSYS APDL (ANSYS Inc. 2012). In the following section, we use four examples to demonstrate the accuracy and efficiency of the algorithm presented here.

4. Application examples

The first three examples presented in this section are of two-dimensional setting while the fourth is a three-dimensional case. A theoretical solution in approximate form exists for the first example, which serves as the guide for validating the accuracy of the proposed algorithm. In the other two examples, the purpose is to demonstrate the efficiency of the numerical algorithm. It is not intended to identify the worst case scenario. Further, the first three examples involve line elements and the last one contains shell elements. It is desirable to first form the stress stiffening matrix in closed form for line elements.

4.1 Stress stiffening matrices of beam elements due to acceleration

The shape function matrix **N** contains the usual linear and Hermite polynomials for bar and beam elements, respectively. Let *L* be the element length, ζ the natural coordinate defined as $\zeta = x/L$, and *x* the axial coordinate. Here only the shape functions for beam elements are given below.

$$\mathbf{N} = [1 - 3\zeta^2 + 2\zeta^3 \quad L(\zeta - 2\zeta^2 + \zeta^3) \quad L(3\zeta^2 - 2\zeta^3) \quad L(-\zeta^2 + \zeta^3)] \tag{19}$$

When the beam is subject to constant acceleration *a* along the axial axis as indicated in Fig. 4, the axial stress in the element appears to be a linear function in *x* as seen below.

$$\sigma_x = \frac{f}{A} \left(\frac{x}{L} - 1 \right) \tag{20}$$

where the inertial force $f = ma = \rho ALa$, *m* the mass of the element, ρ the density and *A* the cross-sectional area. Upon substituting the shape function matrix **N** in Eq. (19) and the axial stress σ_x in Eq. (20) into Eqs. (3) and (4), the stress stiffening matrix **K_a** for an element with nodal coordinates $x_1 < x_2$ and $L = x_2 - x_1$, is given below.

$$\mathbf{K}_a = \frac{f}{60L} \begin{bmatrix} -36 & 0 & 36 & -6L \\ 0 & -6L^2 & 0 & L^2 \\ 36 & 0 & -36 & 6L \\ -6L & L^2 & 6L & -2L^2 \end{bmatrix} + \frac{\sigma_{x_2} A}{30L} \begin{bmatrix} 36 & 3L & -36 & 3L \\ 3L & 4L^2 & -3L & -L^2 \\ -36 & -3L & 36 & -3L \\ 3L & -L^2 & -3L & 4L^2 \end{bmatrix} \tag{21}$$

where σ_{x_2} is σ_x evaluated at $x = x_2$ using Eq. (20). Note the negative diagonal components in the first matrix stem from the positive acceleration. Moreover, the second matrix in essence is the equivalent of stress stiffening on the element by a compressive axial force $-\sigma_{x_2} A$ applied at node 2. If the *x*-displacement is to be included, the matrix can be augmented with ease (Cook *et al.* 2007).

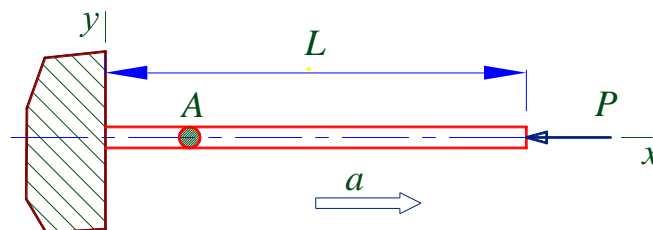


Fig. 4 An elastic beam subject to a constant acceleration force and an axial force *P*

4.2 Buckling of a beam subject to constant acceleration

As depicted in Fig. 4, an elastic beam is subjected to a point force P at the free end as well as constant acceleration a . The theoretical solution of the buckling load when the acceleration is the gravity g is given approximately as follows (Timoshenko and Gere 2009).

$$P_{cr} \approx \frac{\pi^2 EI}{4L^2} - 0.3\rho ALg \quad (22)$$

where EI is the beam's flexural rigidity and L the length of the elastic beam. Note also that the beam would buckle due to its own weight if the following equation holds (Timoshenko and Gere 2009).

$$(\rho ALg)_{cr} \approx \frac{7.837EI}{L^2} \quad (23)$$

We first consider a one-element model with node 1 completely fixed and $\sigma_{x2}=0$ in Eq. (21). Here, each node has three degrees of freedom: two translational displacements, u and v , and one rotation θ . Therefore

$$\left(\begin{bmatrix} \frac{EA}{L} & 0 & 0 \\ 0 & \frac{12EI}{L^3} & -\frac{6EI}{L^2} \\ 0 & -\frac{6EI}{L^2} & \frac{4EI}{L} \end{bmatrix} + \lambda \left(\frac{f}{60L} \begin{bmatrix} 0 & 0 & 0 \\ 0 & -36 & 6L \\ 0 & 6L & -2L^2 \end{bmatrix} + \frac{-P}{30L} \begin{bmatrix} 0 & 0 & 0 \\ 0 & 36 & -3L \\ 0 & -3L & 4L^2 \end{bmatrix} \right) \begin{Bmatrix} u_2 \\ v_2 \\ \theta_2 \end{Bmatrix} \right) = 0 \quad (24)$$

Upon solving the above eigenvalue problem symbolically using MATLAB (MathWorks 2012), we may obtain the dominant eigenvalue λ_1 . Recall $P_{cr}=\lambda_1 P$. Thus, the critical buckling force for the one-element model is

$$P_{cr} = -\frac{\sqrt{10\mu}}{15} + \frac{52}{3}\tau - \frac{1}{3}f \quad (25)$$

where

$$\tau = EI/L^2, \text{ and } \mu = 4960\tau^2 - 20\tau f + f^2. \quad (26)$$

Assuming steel is used ($E=200$ GPa, $\rho=7,890$ kg/m³), acceleration is $a=g=9.81$ m/s² and the geometric properties of a wide-flange beam are: $L=5$ m, $A=1.58 \times 10^{-4}$ m² and $I_{zz}=2.725 \times 10^{-9}$ m⁴, Eq. (25) yields

$$P_{cr} = 35.39 \text{ N} \quad (27)$$

The theoretical solution from Eq. (22) gives $P_{cr} = 35.45$ N which represents an error of about 0.2%.

It is unrealistic to symbolically solve a model with a large number of elements in the similar fashion to Eq. (25). To use the proposed numerical scheme for a twenty-five two-dimensional beam elements for the beam in Fig. 4, a MATLAB code is developed. Note that some of codes in the text by (Kwon and Bang 2000) come handy for this endeavor. In the calculation, the reference

Table 2 Numerical calculation of finding the buckling load for the plane truss in Fig. 5

No.	α	λ	$a, \text{m/s}^2$
1	0.03	173.91	5.2173
2	0.04	167.72	6.7088
3	0.05	161.93	8.0965
4	0.06	156.53	9.3918
5	0.07	151.46	10.6022

In this example, 74 link elements are used for the bars and cables. Each node has two translational degrees of freedom. Three point-elements are used to model the masses at points *D*, *E* and *F*. Table 2 shows the numerical calculation using a code written in MATLAB. Therefore, the target acceleration is enclosed in the interval between $a_4=9.3918$ and $a_5=10.6022$.

Note that the reference load and acceleration are $W=10.0$ KN and $a=1.0$ m/s². From Eqs. (17) and (18), the natural coordinate corresponding to the gravitational acceleration g and the participation factor are, respectively:
 $\xi = 0.3377$ and $\alpha = 0.06338$.

The eigenvalue problem Eq. (9) is solved one final time using $W=10.0$ KN and $\alpha=0.06338$ which results in $\lambda_1=154.78$. The downward acceleration the plane truss subject to is $a=\alpha\lambda_1=9.810$ m/s². And, the buckling load for the beam is: $W_c=W\lambda_1=1547.8$ KN. Note that upon solving the eigenvalue problem from Eq. (1) using the stress stiffening matrix \mathbf{K}_σ of the truss structure stemming from the reference force $W=10.0$ KN and the gravitational acceleration $g=9.810$ m/s², the eigenvalue is $\lambda_1=4.553$. This indicates that the buckling load would have to be $W_c=W\lambda_1=45.53$ KN, which is only 3% of the buckling load using the current algorithm. To cause the truss structure to buckle at this load the gravitational acceleration would have to be $a=g\lambda_1=44.66$ m/s² which is almost four times the actual gravity.

In case the exercise of obtaining α and λ in Table 2 continues until $\alpha=10$, we may have a curve of acceleration vs. participation factor as shown in Fig. 6 which exhibits an asymptote at $a_{\max}=45.69$ m/s². When a large $\alpha \geq 500$ is used in the proposed algorithm, a very small eigenvalue or LF is obtained, e.g., $\lambda_1 \approx 10^{-2}$. This indicates that the structure buckles due to the high acceleration alone and $W_c \approx 0$ KN.

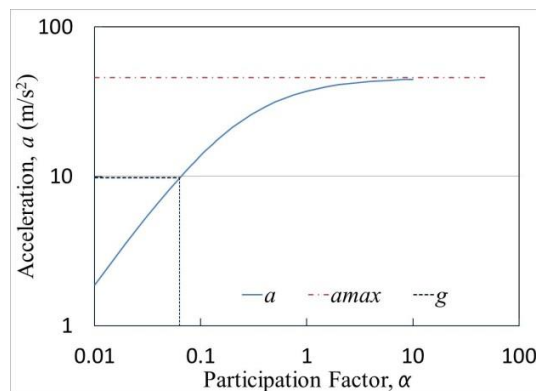


Fig. 6 Plot of acceleration vs. participation factor in logarithmic scale

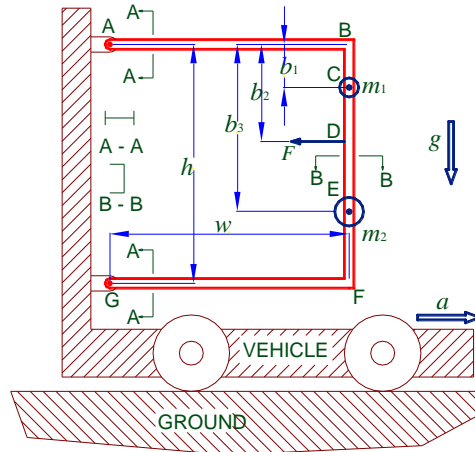


Fig. 7 A traveling vehicle with a plane frame carrying two masses m_1 and mass m_2 and subject to a force F_D

4.4 Buckling of a plane frame on an accelerating vehicle

In the third example, a plane steel ($E=200$ GPa, $\rho=7,870$ kg/m³) frame installed on a vehicle is subject to a known point force $F_D=1,500$ N at point D. In addition there are two known masses $m_1=200$ kg, $m_2=300$ kg at points C and E. The horizontal beams of the frame are of a wide-flange cross-section, while the vertical beam is of C-channel. The cross-sections of beams are: A-A: $A_1=484 \times 10^{-6}$ m² and $I_1=4.205 \times 10^{-8}$ m⁴, and B-B: $A_2=384 \times 10^{-6}$ m², and $I_2=9.260 \times 10^{-8}$ m⁴. It is of interest to know the critical horizontal acceleration a_c of the vehicle when the 2D frame buckles. Note the gravity is $g=9.81$ m/s² and the frame is hinge-supported at points A and G as shown in Fig. 7.

Let us introduce a scaling factor β so that

$$\beta = \frac{F_D}{g} \tag{28}$$

which simply correlates the magnitudes of the two given quantities. Thus, $\beta=152.91$ for the present case. To tackle this example, Eq. (9) is modified to account for the various loads as follows.

$$[\mathbf{K} - \lambda[\alpha g_1(\mathbf{K}_{g_1} + \beta \mathbf{K}_{F_1}) + a \mathbf{K}_a]] \mathbf{U} = \mathbf{0}, \tag{29}$$

where both g_1 and a are arbitrarily chosen magnitudes corresponding to gravity and the horizontal acceleration and $F_1=\beta g_1$. Furthermore, \mathbf{K}_{g_1} , \mathbf{K}_{F_1} and \mathbf{K}_a are, respectively, the individual stress stiffening matrices due to g_1 , F_1 and a alone. The constraint Eq. (10) becomes

$$\alpha g_1 \lambda_1 = g. \tag{30}$$

For the numerical study, the dimensions used for the frame are $h=6$ m, $w=4$ m, $b_1=1.5$ m, $b_2=2$ m and $b_3=4.5$ m. Using $g_1=1$ m/s² and $a=1$ m/s² in the proposed algorithm, the critical participation factor found from Eqs. (17) and (18) is $\alpha_{cr}=1.713$ which is between steps 3 and 4 in Table 3. With this α_{cr} the eigenvalue problem Eq. (29) gives $\lambda_1=5.726$. Therefore

Table 3 Numerical calculation of finding the buckling load for the plane frame in Fig. 7

No.	α	λ	$a, \text{m/s}^2$
1	1.5	6.4605	9.69075
2	1.6	6.094	9.7504
3	1.7	5.7667	9.80339
4	1.8	5.4727	9.85086
5	1.9	5.2072	9.89368



Fig. 8 The first buckle mode of the plane frame in Fig. 7

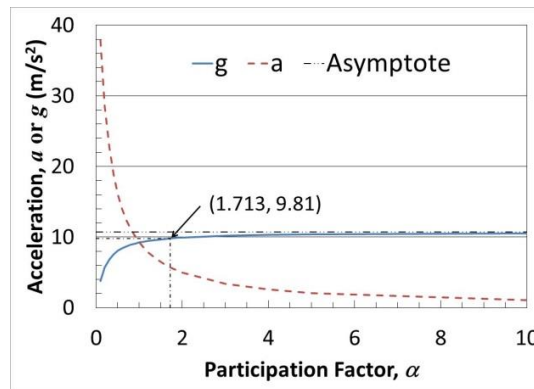


Fig. 9 Plot of acceleration vs. participation factor for the plane frame in Fig. 7

$$\alpha_{cr}g_1\lambda_1 = 9.81 \text{ m/s}^2, F_D = \alpha_{cr}g_1\lambda_1\beta = 1499.77 \text{ N}, \text{ and } a_c = \lambda_1a = 5.726 \text{ m/s}^2. \quad (31)$$

It is seen that constraint Eq. (30) is satisfied. Buckling of the plane frame occurs when the horizontal acceleration is $a_c = 5.726 \text{ m/s}^2$ at which the applied force is exactly as specified, $F_D=1,500 \text{ N}$. The deformed shape of the frame in the first buckling mode is shown in Fig. 8. Note that the setting for this model is not symmetric at all.

Continuation of the computation in Table 3 yields a plot seen in Fig. 9. As expected an asymptote exists $g_{\max}=10.71 \text{ m/s}^2$ at which the horizontal acceleration nearly vanishes, $a_{\min}\approx 0$. That is, the plane frame buckles before the vehicle starts accelerating. Note that the two curves shown in Fig. 9 intersect at $\alpha=1.0$ at which both the horizontal and vertical accelerations are 9.234 m/s^2 . For the frame to buckle at that moment, the applied force is lower than the prescribed load, i.e., $F_D=1,411.9 \text{ N}$.

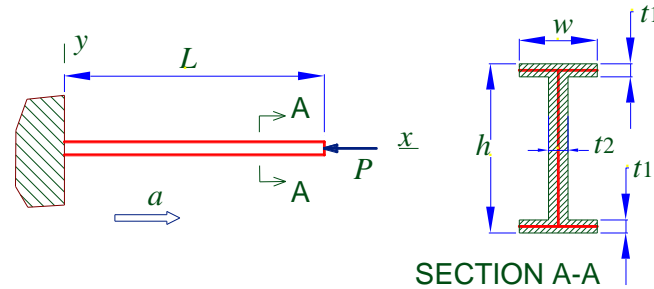


Fig. 10 A wide-flange beam subject to acceleration and axial force

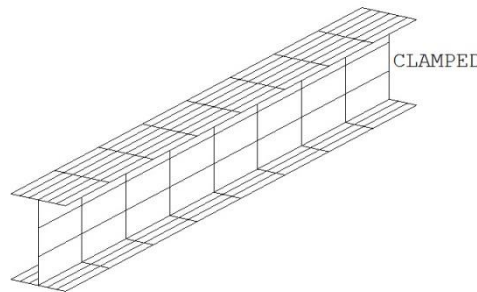


Fig. 11 Finite element model of a wide-flanged beam with clamped end.

4.5 Buckling of a wide-flanged beam clamped at one end

The first example is reexamined here using a beam with Wide Flange cross-section as shown in Fig. 10. Note that the results given in Eqs. (22) and (23) are derived from elementary beam theory (Timoshenko and Gere 2009). The beam in this example is modeled using shell elements with three translational and three rotational degrees-of-freedom per node (Bathe 1996, Cook *et al.* 2007).

Fig. 11 shows a finite element mesh of a short ($L=0.25$ m) wide-flanged beam with an end clamped against any movement. In the numerical demonstrations, the length $L=5.0$ m used for example 1 is considered for consistency. In addition, the material used is steel ($E=200$ GPa, $\nu=0.3$, $\rho=7,890$ kg/m³) and the cross-sectional properties are: $w=0.01$ m, $h=0.03$ m, web and flange thicknesses $t_1=0.002$ m, and $t_2=0.003$ m. This is the setting yielding the cross-sectional area and moment of inertia used in example 1. According to Eq. (23), the beam buckles at the critical acceleration $a_{cr}=27.41$ m/s² when the applied force P is absent. To ensure that the finite element model is accurate, the ordinary buckling problem with inertial force alone is solved. It is found that the critical acceleration $a_{cr}=26.49$ m/s² which represents an error of 3.36%. Two cases are considered in the following numerical demonstration.

4.5.1 Case I: acceleration is given as $a=9.81$ m/s²

In this case the critical buckling force P_{cr} is sought when the beam is subject to acceleration $a=9.81$ m/s². The element aspect ratio as seen in Fig. 11 is maintained throughout, which results in 2685 4-noded shell elements and 3240 nodes. Table 4 shows the numerical calculation following the proposed algorithm. Therefore, the target acceleration is enclosed in the interval between

Table 4 Numerical calculation for finding the participation factor for the beam in Fig. 10 using shell elements

No.	α	λ	$a, \text{m/s}^2$
1	2.2	3.7706	8.29532
2	2.4	3.6689	8.80536
3	2.6	3.5724	9.28824
4	2.8	3.4807	9.74596
5	3.0	3.3935	10.1805

Table 5 Numerical calculation for finding the critical buckling acceleration for the beam in Fig. 10

No.	α	λ	P, N	$a, \text{m/s}^2$
1	1.0	13.555	27.11	13.555
2	1.2	12.331	29.5944	12.331
3	1.4	11.309	31.6652	11.309
4	1.6	10.441	33.4112	10.441
5	1.8	9.6963	34.9067	9.6963
6	2.0	9.05	36.2	9.05

$a_4=9.74596$ and $a_5=10.1805$. From Eqs. (17) and (18) the natural coordinate corresponding to the given acceleration and the participation factor are, respectively:

$$\xi = 0.14409 \text{ and } \alpha = 2.8288.$$

Using the critical participation factor $\alpha_{cr}=2.8288$ and the reference values $P=10 \text{ N}$ and $a=1 \text{ m/s}^2$, the eigenvalue problem Eq. (9) is solved. The critical load factor found is $\lambda_1=3.4679$. Thus the constraint equation Eq. (10) is satisfied, $\alpha_{cr}a\lambda_1=2.8288 \times 1 \times 3.4679=9.81$. The beam then buckles at $P_{cr}=P\lambda_1=34.679 \text{ N}$, which is in good agreement (error=2.2 %) with the theoretical solution using elementary beam theory, $P_{cr} = 35.45 \text{ N}$.

4.5.2 Case II: applied axial force is given as $P_0=30 \text{ N}$

We will now use the proposed algorithm to determine the critical acceleration a_{cr} when the applied force at the free end of the beam is $P_0=30 \text{ N}$. To this end, the CEVP is modified as follows.

$$[\mathbf{K} + \lambda(\alpha\mathbf{K}_P + \mathbf{K}_a)]\mathbf{U} = \mathbf{0} \quad (32)$$

subject to

$$\alpha P \lambda_1 = P_0 \quad (33)$$

Now the constraint equation with unknown participation factor is imposed on the applied axial force P .

As in the previous situation, a and P hold arbitrary reference values which are chosen as $a=1.0 \text{ m/s}^2$ and $P=2 \text{ N}$. Further, the value of the participation factor is iterated between $1 \leq \alpha \leq 12$ some of which are given in Table 5 below with sufficient steps for computing the participation factor corresponding to P_0 . Here an additional column for a is included in the table.

Using $P_2=29.5944$ and $P_3=31.6652$ in place of a_i in Eqs. (17) and (18) the natural coordinate and the participation factor corresponding to the given applied force P_0 are, respectively:

$$\xi = 0.1811 \text{ and } \alpha = 1.2362.$$

Upon solving Eq. (32) using $\alpha=1.2362$, we have $\lambda_1=12.133$. Thus the constraint Eq. (33) is

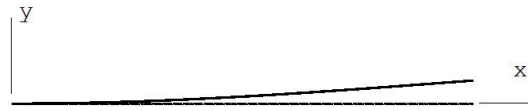


Fig. 12 First buckling mode of the wide-flanged beam

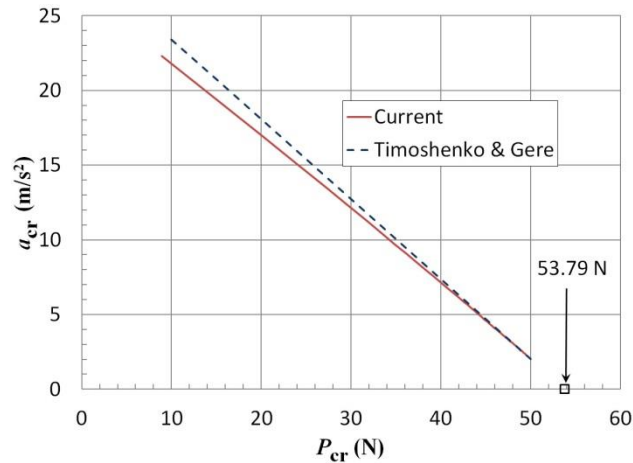


Fig. 13 Critical acceleration vs. applied force predicted by the current algorithm and theoretical solution

satisfied, $\alpha P \lambda_1 = 29.998$ and the critical acceleration for buckling is $a_{cr} = a \lambda_1 = 12.133 \text{ m/s}^2$. Note that Eq. (22) can be rewritten as below.

$$a_{cr} \approx \frac{1}{0.3 \rho A L} \left(\frac{\pi^2 E I}{4 L^2} - P_0 \right) \tag{34}$$

It allows us to calculate the theoretical solution for the critical acceleration, $a_{cr} = 12.724 \text{ m/s}^2$. The proposed algorithm appears to be in good agreement (error=2.2 %) with the theoretical solution. Further, at this critical situation, the beam’s buckling shape is shown in Fig. 12 which coincides with the prediction using elementary beam theory.

Fig. 13 depicts the plot of the last two columns of Table 5 using extended range of α , $1 \leq \alpha \leq 12$, together with the linear theoretical solution, Eq. (34). It is seen that both lines converge to the point representing the critical buckling load of the fixed-free beam without acceleration, $P_{cr} = 53.79 \text{ N}$, the first term in Eq. (22), or the Euler buckling load.

5. Conclusions

The determination of the buckling load of an elastic structure in the presence of inertial force is formulated as an eigenvalue problem subject to an equality constraint correlating an unknown participation factor and the acceleration. A methodology of solving the constrained eigenvalue problem is presented. In the numerical algorithm, the eigenvalue problem is solved incrementally until the desired participation factor falls within an interval. Interpolation is employed to extract the accurate solution for the unknown participation factor. The eigenvalue problem is solved again

using the participation factor found. Four examples are used to demonstrate the accuracy of the numerical algorithm. Among them, one has an approximate theoretical solution. The solution predicted by the proposed algorithm is in excellent agreement with the theoretical solution. From the other two examples involving two-dimensional truss and frame, it is shown that the critical buckling loads predicted from the proposed algorithm are lower than those from the usual procedure by a relatively significant margin. The fourth example contains shell elements used to model a wide-flange beam. The procedure involves some laborious manual intervention. It is necessary to develop an automatic numerical scheme for the problem in the future.

Acknowledgements

Wenjing Wang is grateful to the support from the National Natural Science Fund Committee. The second author (R. Gu) is grateful to the support provided by Beijing Jiaotong University, China, for his visiting professorship under an international program administered by Professor Zhiming Liu, Associate Dean, School of Mechanical, Electric and Control Engineering and Dr. Xinhua Deng, Director, Office of International Cooperation and Exchange.

The work is supported by National Natural Science Funds of China (Grant No. 51205017).

References

- ABAQUS User Documentation, v. 6.9. (2011), Simulia, Providence, RI, USA.
- ADINA Theory & Modeling Guide (2012), ADINA R & D Inc., Watertown, MA, USA.
- ANSYS User's Manual (2012), v. 14, ANSYS Inc., Canonsburg, PA, USA.
- Bathe, K.J. (1996), *Finite Element Procedures*, Prentice Hall, Upper Saddle River, NJ, USA.
- Carrera, E., Lecca, S., Nali, P. and Soave, M. (2011), "Influence of in-plane axial and shear loading on the vibration of metallic plates", *Int. J. Appl. Mech.*, **3**(3), 447-467.
- Chajes, A. (1974), *Principles of Structural Stability Theory*, Prentice-Hall, Englewood Cliffs, N.J., USA.
- Cheng, Z.Q., Reddy, J.N. and Xiang, Y. (2005), "Buckling of a thin circular plate loaded by in-plane gravity", *J. Appl. Mech.*, **72**, 296-298.
- Cook, R.D., Malkus, D.S., Plesha, M.E. and Witt, R.J. (2007), *Concepts and Applications of Finite Element Analysis*, 3rd Edition, Wiley, Hoboken, NJ, USA.
- Dougherty, B.K. (1990), "Stability of beams subject to combined gravity loading and applied end moments", *Proc. Instn Civil Eng.*, Part 2, **89**, 241-250.
- Dougherty, B.K. (1991), "The elastic buckling of beams under mixed gravity loading", *Struct. Eng. London*, **69**(2), 25-28.
- Hernandez-Urrea, J.A., Uribe-Henao, A.F. and Aristizabal-Ochoa, J.D. (2014), "Stability and free vibration analyses of cantilever shear buildings with semi-rigid support conditions and multiple masses", *J. Sound Vib.*, **333**(5), 1390-1407.
- Cui, H.L. and Shen, H.S. (2011), "Modeling and simulation of buckling and postbuckling of plant stems under combined loading conditions", *Int. J. Appl. Mech.*, **3**(1), 119-130.
- Kerstens, J.G.M. (2005), "A review of methods for constrained eigenvalue problems", *Heron*, **50**(2), 109-132.
- Kumar, A. and Healey, T.J. (2010), "A generalized computational approach to stability of static equilibria of nonlinearly elastic rods in the presence of constraints", *Comput. Meth. Appl. Mech. Eng.*, **199**, 1805-1815.
- Kwon, Y.W. and Bang, H. (2000), *The Finite Element Method Using MATLAB*, 2nd Edition, CRC Press, FL, USA.

- MARC (2013), *Volume A: Theory and User Information*, MSC Software, Santa Ana, CA, USA.
- MATLAB, The MathWorks Inc., Natick, MA, USA.
- Roberts, T.M. and Azizian, Z.G. (1984), "Instability of monosymmetric I-beams", *J. Struct. Eng., Proc. ASCE*, **110**(6), 1415-1419.
- Roberts, T.M. and Burt, C. (1985), "Instability of monosymmetric I-beams and cantilevers", *Int. J. Mech. Sci.*, **27**(5), 313-324.
- Silvestre, N., Faria, B. and Duarte, A. (2012), "Multilevel approach for the local nanobuckling analysis of CNT-based composites", *Coupl. Syst. Mech.*, **1**(3), 269-283.
- Timoshenko, S. and Gere, J. (2009), *Theory of Elastic Stability*, 2nd Edition, Dover Publications, New York, NY, USA.
- Wang, X., Lu, G. and Lu, Y.J. (2007), "Buckling of embedded multi-walled carbon nanotubes under combined torsion and axial loading", *Int. J. Solid. Struct.*, **44**(1), 336-351.
- Yamada, S., Ishida, T., Shimada, Y. and Matsunaga, T. (2013), "Cyclic loading test on RHS columns under bi-directional horizontal forces", *J. Struct. Construct. Eng.*, **78**(683), 203-212.
- Yanagisawa, D., Nagai, K.I. and Maruyama, S. (2008), "Effects of axial compressive load on chaotic vibrations of a clamped-supported beam", *Tran Japan Soc. Mech. Eng., Part C*, **74**(5), 1073-1079.
- Zhou, M. (1995), "An efficient DCOC algorithm based on high-quality approximations for problems including eigenvalue constraints", *Comput. Meth. Appl. Mech. Eng.*, **128**, 383-394.

CC